Journal of the Korean Physical Society, Vol. 72, No. 5, March 2018, pp. 593∼598

Annealing Temperature Dependent Structural and Magnetic Properties of Ni−Cu−Zn Nanoferrites

P. Venkata Srinivasa Rao*
Department of Physics, Acharya Nagarjuna University, Guntur 522510, India and
Department of Physics, S. S. N. College, Guntur 522601, India

T. Anjaneyulu
Department of Physics, Narasaraopet Engineering College, Narasaraopet 522601, India

M. Rami Reddy
Department of Physics, Acharya Nagarjuna University, Guntur 522510, India

(Received 10 October 2017, in final form 10 November 2017)

The effect of annealing temperature on the structural and the magnetic properties of $Ni_{0.5}Cu_{0.25}Zn_{0.25}Fe_2O_4$ (Ni−Cu−Zn) nanoferrites synthesized using an oxalic-based precursor method was investigated in detail. A single phase of the Ni−Cu−Zn ferrite was observed from X-ray diffraction (XRD) data. From the XRD analysis, the grain size was found to increase with increasing annealing temperature from 500 to 800 °C whereas the lattice constant was found to decrease. The scanning electron microscope (SEM) analysis showed nanosize grains in the prepared samples. The magnetization analysis showed that the saturation magnetization (M_s) increased with increasing annealing temperature due to the increasing grain size whereas the coercivity (H_c) and the remanence magnetization (M_r) showed decreasing behaviors. The Curie temperature (T_C) was measured for all samples. As the grain size increased the Curie temperature was also observed to increase. For these samples, the Curie temperatures lies between 426 K to 504 K. The dielectric constant (ε') was observed to be higher for these samples. The dielectric loss tangent increase slowly with increasing frequency till a particular frequency, after that it slowly decreased. Therefore the annealing temperature was observed to have a significant effect on the structural, magnetic and electrical properties of synthesized Ni−Cu−Zn ferrite.

PACS numbers: 77.22.−d, 77.22.Gm
Keywords: Ni−Cu−Zn nanoferrites, Structural properties, Magnetic properties, Electrical properties
DOI: 10.3938/jkps.72.593

I. INTRODUCTION

Spinel Ni−Cu−Zn ferrites have attracted attention during recent years because of their wide applications in surface-mounted technology as ferrite inductors incorporated into a printed circuit board [1]. Ni−Cu−Zn ferrites are the key materials in multi-layer chip inductors (MLCIs) due to their high permeability, excellent magnetic properties, high electrical stability, environmental stability *etc.* [2, 3]. Research on the application of Ni−Cu−Zn ferrites in MLCIs is growing as these oxides can be sintered and synthesized at low temperatures [1,4–6]. Ni−Cu−Zn ferrites have also been found to have wide applications in electronic devices such as mobile phones, cameras, computers, *etc.* [7]. In the past, Ni−Cu−Zn nanoferrites were synthesized using different techniques [8–10], under different annealing temperatures [11–13] and by adding different doping elements [8, 9, 14–18] to tailor their physical and chemical properties at low temperatures. The synthesis technique was observed to play an important role in improving the physical properties of Ni−Cu−Zn nanoferrites. Therefore, in this present work, we used an oxalic acid-based precursor method [19–21] to fabricate Ni−Cu−Zn nanoferrites, and we investigate their structural, magnetic and electrical properties.

II. EXPERIMENTAL PROCEDURE

$Ni_{0.5}Cu_{0.25}Zn_{0.25}Fe_2O_4$ (Ni−Cu−Zn) ferrite nanopowders were synthesized using an oxalate-based precursor method [19–21]. All the chemicals used were a.r. grade from Sigma-Aldrich and had purities $\geq$ 99%. In this synthesis process, nickel nitrate hydrate

*E-mail: pvsrinivasphd@gmail.com

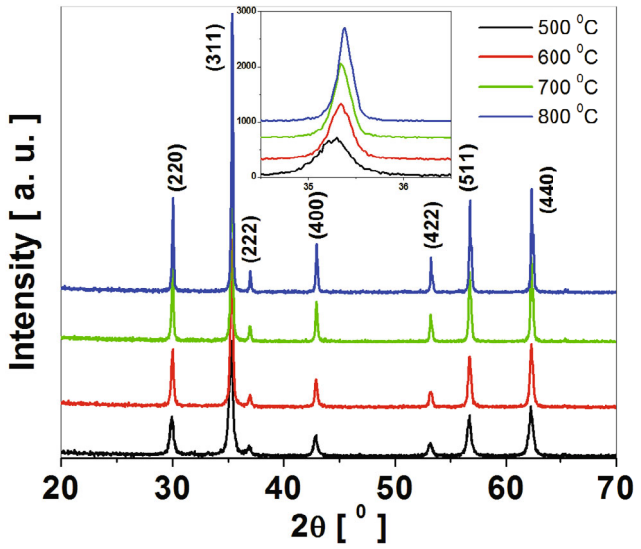

Fig. 1. (Color online) X-ray diffraction patterns of $Ni_{0.5}Cu_{0.25}Zn_{0.25}Fe_2O_4$ samples annealed from 500 to 800 °C. Inset of figure shows expanded curve (311) peak.

$(Ni(NO_3)_2.6H_2O)$, cupric nitrate hydrate $(Cu(NO_3)_2 \cdot 6H_2O)$, zinc nitrate hydrate $(Zn(NO_3)_2 \cdot 6H_2O)$ and ferric nitrate nonahydrate $(Fe(NO_3)_3.9H_2O)$ were used as the starting materials. The entire synthesis process is described elsewhere [19]. The resultant mixtures were evaporated on a hot plate at $\sim$ 150 °C for 2 h. The obtained raw powders were thermally heat treated at 450 °C for 4 h.

The structural properties of the obtained ferrite powders was measured using Phillips X-ray diffraction (XRD) with a Ni filter and Co Kα radiation (λ = 1.78894 Å). The average grain size (D) was calculated using the most intense peak, the (311) peak by employing the Scherrer formula. Scanning electron microscope (SEM) analyses were performed by using a Philips CM-12 scanning electron microscope attached to an energy dispersive X-ray spectrometer (EDS). EDS measurement was carried to further confirm the composition of the prepared samples. The room temperature magnetic properties were measured with a vibrating sample magnetometer (VSM 4500), and the Néel temperatures were measured by applying a small magnetic field of 20 Oe. The dielectric properties were measured using a Nova Control, Alpha high performance frequency analyzer.

III. RESULTS AND DISCUSSION

The X-ray diffraction patterns of $Ni_{0.5}Cu_{0.25}Zn_{0.25}Fe_2O_4$ ferrites annealed at temperature from 500 to 800 °C are shown in Fig. 1. The XRD patterns clearly indicate the formation of a single-phase spinel structure without any secondary phases. The obtained lattice constants are nearly in agreement with the standard values as reported in literature [19]. With increasing annealing temperature, the XRD peak is observed to become sharper. The decrease in the full width at half maximum is evidence of increasing particle size, as shown in Table 1. The lattice constant decreases slightly with increasing annealing temperature. As observed from Fig. 1, the intensity of the diffraction lines is increasing, and the peaks are shifting towards higher 2θ angles. The changes in the lattice constant are due to the small difference between the ionic radii of Ni^{2+} and Fe^{3+}. The ionic radius of Ni^{2+}

Table 1. Dependence of lattice constant (a), grain size (D), coercivity (H_c), remanence magnetization (M_r) and saturation magnetization (M_s) and Curie temperature (TN) on the annealing temperature of $Ni_{0.5}Cu_{0.25}Zn_{0.25}Fe_2O_4$ nanoparticles.

Temperature (°C)	a (Å)	D (nm)	H_c (Oe)	M_r (emu/g)	M_s (emu/g)	T_C (K)
500 °C	8.421	27	202	11.8	38.6	426
600 °C	8.419	33	113	8.9	42.8	445
700 °C	8.415	39	91	7.3	50.4	488
800 °C	8.411	45	36	4.3	55.4	504

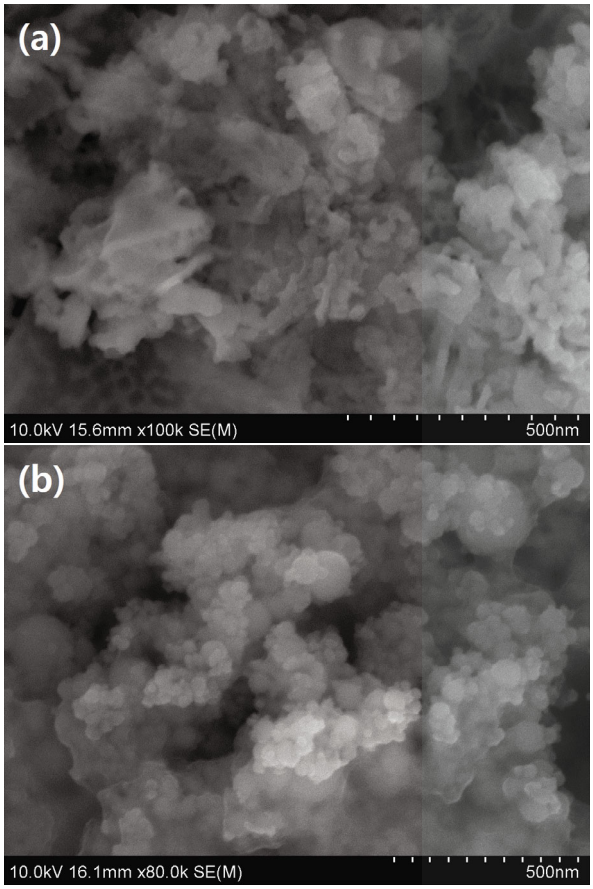

Fig. 2. SEM images of $Ni_{0.5}Cu_{0.25}Zn_{0.25}Fe_2O_4$ samples annealed at (a) 500 °C and (b) 800 °C.

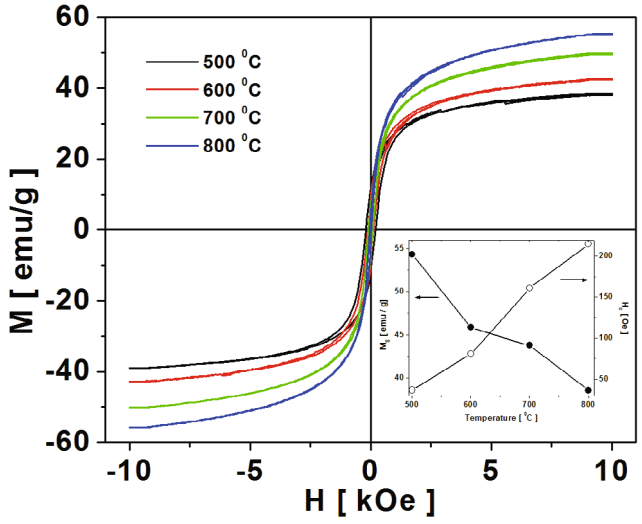

Fig. 3. (Color online) M-H curves of $Ni_{0.5}Cu_{0.25}Zn_{0.25}Fe_2O_4$ samples annealed from 500 to 800 °C. Inset of figure shows dependence of saturation magnetizing (M_s) and coercivity (H_c) on annealing temperature of $Ni_{0.5}Cu_{0.25}Zn_{0.25}Fe_2O_4$ samples.

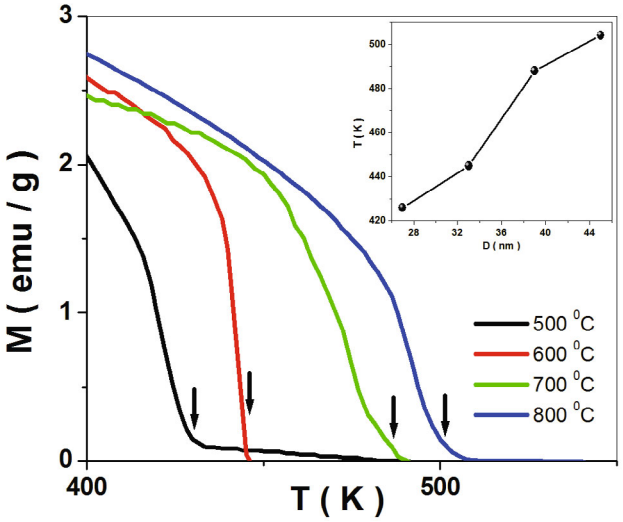

Fig. 4. (Color online) Magnetization vs. temperature for $Ni_{0.5}Cu_{0.25}Zn_{0.25}Fe_2O_4$ samples measured by applying small magnetic field for different grain sizes. Vertical arrows designate T_C. Inset of figure shows Néel temperature vs. average particle size for $Ni_{0.5}Cu_{0.25}Zn_{0.25}Fe_2O_4$ samples.

(0.69 A°) and that of Fe^{3+} (0.67 A°) are very near to each other. Due to this small difference, the lattice constant was not largely affected. Such kind of similar behavior was observed in the $Ni_{0.5+1.5x}Cu_{0.3}Zn_{0.2}Fe_{2-x}O_4$ ferrite synthesized using the oxalic-acid-based precursor method [19]. Evidence in literature confirms that the lattice constants and the grain size are directly related. From our investigations, we observed that the lattice parameters continue to decrease slightly with increasing the grain size.

Figures 2(a) and (b) show the SEM micrographs of $Ni_{0.5}Cu_{0.25}Zn_{0.25}Fe_2O_4$ ferrite nanoparticles annealed at 500 and 800 °C respectively. The micrographs show the nanosize grains in the synthesized samples, as well as slight agglomerations among particles due to smaller grain sizes in the prepared samples. The SEM images also illustrate that the grain size increases with increasing annealing temperature. The EDS spectra of the $Ni_{0.5}Cu_{0.25}Zn_{0.25}Fe_2O_4$ samples confirmed the existence of elemental Ni, Cu, Zn, Fe and O in our prepared samples, which agrees very well with the results of the XRD analysis.

The effect of annealing temperature on the magnetic properties of $Ni_{0.5}Cu_{0.25}Zn_{0.25}Fe_2O_4$ ferrites are shown in the plot of magnetization versus magnetic field $M(H)$ (see Fig. 3). All samples showed the typical behavior of soft magnetic materials. The magnetic properties, such as the saturation magnetization (M_s), remanence (M_r) and coercivity (H_c), are strongly linked to the grain size and the crystal structure. In nanoparticles, finite size, surface disorders and interparticle interactions were observed to possibly have a strong influence on the magnetic properties. In nanostructured materials, the increase in surface spins will have a strong influence on the magnetic properties. The short or long-range atomic ordering in magnetic materials also has its own effect on the magnetic properties.

With increasing annealing temperature, the value of M_s was observed to be enhanced significantly, as shown in the inset of Fig. 3. For instance, the value of M_s for the sample annealed at 500 °C was found to be 38.6 emu/g, and that value increased to 55.4 emu/g when the sample was annealed at 800 °C. The enhancement due to annealing was found to be 44%. The enhancement of M_s could be attributed to the increased grain size. Therefore, in the present case, the annealing temperature had a significant effect on the magnetic properties of $Ni_{0.5}Cu_{0.25}Zn_{0.25}Fe_2O_4$ ferrite nanoparticles. A similar kind of magnetic behavior was reported for ferrites with different compositions synthesized by using other methods [22]. The magnetic properties are also well known to depend on the synthesis techniques and the conditions. In the case of the remanence magnetization and the coercivity, the trends were different. They both decreased with increasing the annealing temperature, as mentioned in Table 1. The decrease in the coercivity in the present study might be due to the multidomain nature of the samples at higher annealing temperatures [23,24] whereas the enhancement in the coercivity is usually a typical feature of a canted magnetic structure [25]. Due to the higher magnetization in these ferrites, they can be used as loud speakers, refrigerator magnets, brakes *etc.*, as well as in musical instruments. Therefore, they have an advantage over other magnets due to their excellent demagnetization resistance, huge corrosion resistance and low cost; the disadvantage of these ferrites

is that they are brittle in nature. The low coercivity in these ferrites is useful in reducing the eddy current losses and makes magnetizing and demagnetizing easy in these magnetic materials for industrial applications.

The Curie temperatures for the $Ni_{0.5}Cu_{0.25}Zn_{0.25}Fe_2O_4$ ferrite samples were measured with a small applied field of 20 Oe, and the results are shown in Fig. 4. The observed Curie temperature values for all the $Ni_{0.5}Cu_{0.25}Zn_{0.25}Fe_2O_4$ ferrite samples are presented in Table 1. Figure 4 shows the spontaneous change in the magnetization with increasing temperature. The observed Curie temperatures for our samples were found to be nearly equal to those of other Ni−Cu−Zn Ferrite samples. From Fig. 4 (see inset), the Curie temperature is observed to increase with increasing grain size. Earlier, an increase in the Curie temperature with increasing grain size was observed for $MnFe_2O_4$ and $NiFe_2O_4$ nanomaterials [26–29]. From Fig. 4, as the temperature increases, the magnetization is observed to remain constant up to a certain temperature, after which it falls slowly until the magnetization becomes zero. The temperature at which the sample loses its magnetization is known as the Curie temperature (T_C). At this temperature, the materials transform from a ferrimagnetic phase to a paramagnetic phase. For our samples, the measured Curie temperatures lie between 426 K to 504 K. As the grain size increased, the Curie temperature was also observed to increase. A low Curie temperature ferrite material may be used in the construction of thermostats to record the measurement activity of radioactive isotopes [28].

The Curie temperature is also used to identify the amount of magnetic interaction present in the sample and it depends on the size of the grain or particle or on the formula unit. Samples with higher Curie temperatures were observed to have stronger magnetic interaction, as evidenced from Fig. 3. In the present case, the grain size was observed to increase with increasing annealing temperature; therefore, higher grain sizes may require more thermal energy to suppress the spin alignment in the samples. These results are in good agreement with those of the previous studies [27–30].

The dielectric behavior among ferrites is considered to be one of the important properties that predominantly depend on the synthesis/preparation technique, annealing time, annealing temperature and type of dopant and its quantity. The variations in the dielectric constant (ε') with frequency for Ni−Cu−Zn ferrites are shown in Fig. 5(a). All the samples are observed to exhibit dielectric dispersion. The dielectric constant was observed to decrease initially with increasing frequency and then to become almost constant at higher frequencies. Different grain sizes show different dielectric constants but the behaviors are same. At a certain frequency, all the samples show a frequency-independent behavior which may be explained using the well-known Maxwell-Wagner-type interfacial polarization, which is in agreement with Koop's phenomenological theory [31–33]. The dielectric polarization among ferrites is similar to that of the conduction hopping mechanism. Hopping of electrons between Fe^{2+} and Fe^{3+} in the direction of the applied field occurs and determines the polarization. The polarization decreases with increasing frequency and then reaches a constant value. This is based on the fact that beyond a certain applied frequency, the electron exchange between $Fe^{2+} \leftrightarrow Fe^{3+}$ may not follow alternating electric field. The larger dielectric constants at lower frequencies may be due to the predominance of Fe^{2+} ions, interfacial dislocations, grain boundary defects, oxygen vacancies [19,31,32]. The decrease in the dielectric constant (ε') with increasing frequency is a natural phenomenon due to the fact that any element contributing to polarization will show a lagging effect with the applied field at some higher frequencies.

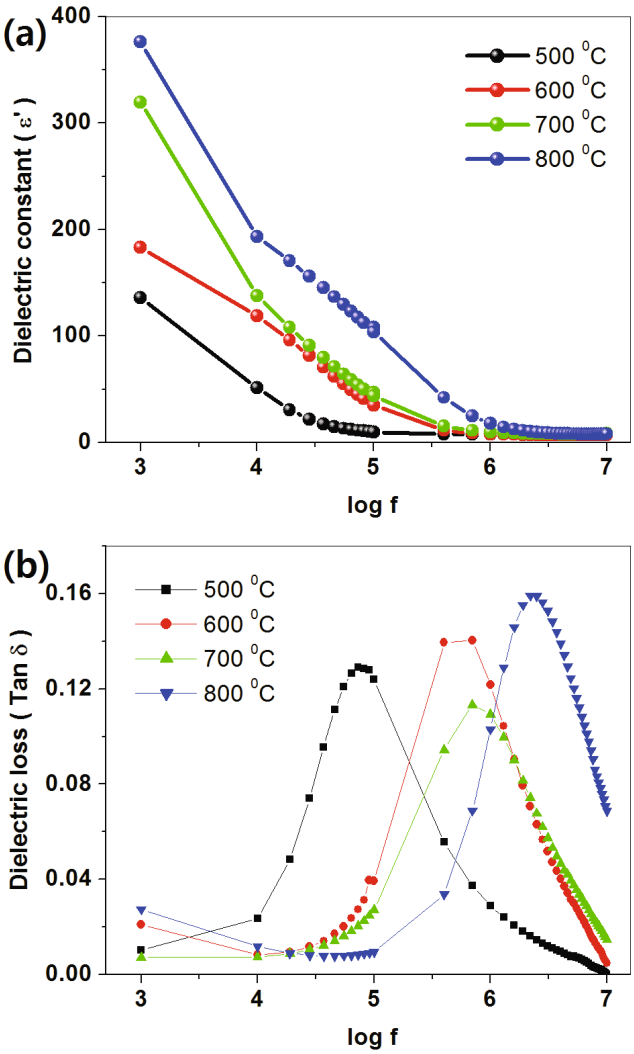

Fig. 5. (Color online) (a) Variation of dielectric constant with frequency for $Ni_{0.5}Cu_{0.25}Zn_{0.25}Fe_2O_4$ samples annealed from 500 to 800 °C, (b) Variation of dielectric loss tangent with frequency for $Ni_{0.5}Cu_{0.25}Zn_{0.25}Fe_2O_4$ samples annealed from 500 to 800 °C.

The observed dielectric constant values for our Ni−Cu−Zn ferrite samples are little more than those reported for Ni−Cu−Zn ferrite synthesized by using different processes and different compositions. The conduction mechanism among the ferrites is mainly due to the hopping of electrons between ions of the same element with different oxidation states. The lower dielectric constant values are observed among ferrites that are annealed at lower temperatures due to the low possibility of ions existing in different valance states which reduces the probability of hopping electrons [19,34]. Also, the grain/ particle size, density, stoichiometry and homogeneity of the ferrites are observed to affect the dielectric constant values [35]. Therefore, as our samples are annealed at higher temperatures, the dielectric constants are observed to be more.

The dielectric loss tangent ($\tan\delta$) as a function of applied frequency at room temperature was investigated. The dielectric loss tangent data plotted in Fig. 5(b) clearly shows that for all the samples the dielectric loss tangent increases slowly with the increase of frequency till a particular frequency, after which it slowly decreases. Different grain sizes show different dielectric loss tangent curves and different values. The appearance of a resonance peak at a particular frequency in all the samples can be interpreted as follows: Imagine that an ion having more than one equilibrium position, as an example consider two positions named A and B having equal potential energies which are separated by a potential barrier, the jumping probability of ions from A to B and from B to A will be similar. Based on the probability, ions exchange positions between the two states with some frequency, called the natural jumping frequency between the two positions. With the application of an external alternating field having the same frequency, the maximum electrical energy will be transferred to the oscillating ions; due to this, the power loss in the ferrites rises, thereby resulting in a resonance according to Debye relaxation theory [19,36]. The peaks in the dielectric loss tangent appear when the applied field time is in phase with the dielectric and when the condition $\omega\tau = 1$ is satisfied, where $\omega = 2\pi f$, f being the frequency of the applied field and τ being the relaxation time, which is related to the jumping probability per unit time p by the equation $\tau = p/2$; *i.e.*, the peak frequency ($f_{\max}$) is proportional to the jumping probability. With an increase in $f_{\max}$ and in the annealing temperature, the hopping or jumping probability increases per unit time.

IV. CONCLUSION

The $Ni_{0.5}Cu_{0.25}Zn_{0.25}Fe_2O_4$ ferrite nano powders were successfully synthesized using the oxalic based precursor method. The XRD analysis confirmed that with increasing annealing temperature, the grain size increased and the lattice constant decreased. The SEM analysis showed nanosize grains in the prepared samples. The magnetization analysis showed that with increasing annealing temperature, the M_s increased whereas the coercivity (H_c) and the remanence magnetization (M_r) showed decreasing behavior. The observed magnetic properties were directly related to the increase in the grain size due to the annealing temperature. The Curie temperature (T_C) was observed to increase with increasing grain size and to lie between 426 K to 504 K. The dielectric constant (ε') for these samples was observed to be a little higher than for other Ni−Cu−Zn ferrite samples. The dielectric loss tangent was found to increase slowly with increasing frequency until a particular frequency, after which it slowly decreased.

ACKNOWLEDGMENTS

The authors thank the Sophisticated Analytical Instrumentation Facility (SAIF), Indian Institute of Technology (IIT) Madras, for measurements. P. S. R. thanks UGC, government of India, for granting a scholarship under the faculty development program (FDP).

REFERENCES

[1] M. Sugimoto, J. Am. Ceram. Soc. **82**, 80 (1999).
[2] Y. Wang, H. Zhou, H. Qi, L. Ren, Z. Xu and Z. Ye, Ceram. Int. **41**, 12253 (2015).
[3] H. K. Zhu, Y. Jin, H. O. Zhu, W. Shen, Y. Q. Xu and H. Q. Zhou, Mater. Res. Bull. **61**, 32(2015).
[4] S-F. Wang, Y-F. Hsu, Y-X. Liu and C-K. Hsieh, J. Magn. Magn. Mater. **394**, 470 (2015).
[5] J. Murbe and J. Topfer, J. Electro-Ceram. **15**, 215 (2015).
[6] L. Z. Li, L. Peng, X. H. Zhu and D. Y. Yang, J. Electron. Sci. Technol. **10**, 88 (2012).
[7] I. Z. Rahman, and T. T. Ahmed, J. Magn. Magn. Mater. **290**, 1576 (2005).
[8] M. A. Gabal, A. M. Asiri and Y. M. Al Angari, Ceram. Int. **37**, 2625 (2011).
[9] K. Praveena, K. Sadhana, S. Srinath and S.R. Murthy, J. Phys. Chem. Solids **74**, 1329 (2013).
[10] A. Xia, C. Jin, D. Du and G. Zhu, J. Magn. Magn. Mater. **323**, 1682 (2011).
[11] N. N. Cheng, Z. Wang and T. T. Liu, IEEE Trans. Magn. **49**, 4188 (2013).
[12] M. P. Reddy, I. G. Kim, D. S. Yoo, W. Madhuri, N. R. Reddy, K. V. S. Kumar and R. R. Reddy, Mater. Sci. Appl. **3**, 628 (2012).
[13] H. Su, X. Tang, H. Zhang, Y. Jing, F. Bai and Z. Zhong, J. Appl. Phys. **113**, 17B301 (2013).
[14] B. D. Ingale and M. A. Barote, J. Chem. Biol. Phys. Sci. **3**, 2801 (2013).
[15] H. Su, H. Zhang, X. Tang and X. Xiang, J. Magn. Magn. Mater. **283**, 157 (2004).
[16] T. Y. Byun, S. C. Byeon and K. S. Hong, IEEE Trans. Magn. **35**, 3445 (1999).

[17] A. Lucas, R. Lebourgeois, F. Mazaleyrat and E. Labouré, Appl. Phys. Lett. **97**, 182502 (2010).
[18] J. Kato, K. Ono and Y. Matsuo, Mater. Sci. Eng. **18**, 092012 (2011).
[19] A. T. Raghavender, Sagar E. Shirsath and K. Vijaya Kumar, J. Alloys Comp. **509**, 7004 (2011).
[20] D. G. Wickham, Inorg. Synth. **9**, 152 (1967).
[21] N. D. Chaudhari, R. C. Kambale, J. Y. Patil, S. R. Sawant and S. S. Suryavanshi, Mater. Res. Bull. **45**, 1713 (2010).
[22] M. Rajendran, R. C. Pullar, A. K. Bhattacharya, D. Das, S. N. Chintalapudi and C. K. Majumdar, J. Magn, Magn. Mater. **232**, 71 (2001).
[23] X. Huang and Z. Chen, J. Magn. Magn. Mater. **280**, 37 (2004).
[24] M. George, S. S. Nair, A. M. John, P. A. Joy and M. R. Anantharamam, J. Phys. D **39**, 900 (2006).
[25] R. H. Kodama, A. E. Berkowitz, E. J. McNiff and S. Foner, Phys. Rev. Lett. **77**, 394 (1996).
[26] J. P. Chen, C. M. Sorensen, K. J. Klabunde, G. C. Hadjipanayis, E. Devlin and A. Kostikas, Phys. Rev. B **54**, 9288 (1996).
[27] C. N. Chinnasamy, A. Narayanasamy, N. Ponpandian, R. Justin Joseyphus, B. Jeyadevan, K. Tohji and K. Chattopadhyay, J. Magn. Magn. Mater. **238**, 281 (2003).
[28] G. Almassy, L. Tardos, Budapest XI., Stoczek u. 2, Hungary.
[29] A. T. Raghavender and N. H. Hong, J. Magn. Magn. Mater. **323**, 2145 (2011).
[30] S. G. Bachhav, R. S. Patil, P. B. Ahirrao, A. M. Patil and D. R. Patil, Mater. Chem. Phys. **129**, 1104 (2011).
[31] J. C. Maxwell, *A Treatise on Electricity and Magnetism* (Oxford, New York, 1954), Vol. 2.
[32] K. W. Wagner, Ann. Phys. **40**, 817 (1913).
[33] C. G. Koops, Phys. Rev. **83**, 121 (1951).
[34] M. P. Reddy, W. Madhuri, G. Balakrishnaiah, N. R. Reddy, K. V. Siva Kumar, V. R. K. Murthy and R. R. Reddy, Curr. Appl. Phys. **11**, 191 (2011).
[35] T. T. Ahmed, I. Z. Rahman and M. A. Rahman, J. Mater. Process. Technol. **153**, 797 (2004).
[36] G. R. Kumar, Y. C. Venudhar, A. T. Raghavender and K. V. Kumar, J. Korean Phys. Soc. **60**, 1082 (2012).